

Density-functional study of water adsorption on the $\text{PuO}_2(110)$ surface

Xueyuan Wu and Asok K. Ray*

Department of Physics, P.O. Box 19059, University of Texas at Arlington Arlington, Texas 76019-0059

(Received 4 June 2001; published 30 January 2002)

Water adsorption on a $\text{PuO}_2(110)$ surface is studied using a periodic model with both the local-density approximation (LDA) and the generalized gradient approximation (GGA) of density-functional theory. The 60 core electrons of the Pu atom are represented by a relativistic effective core potential, and scalar relativistic effects have been incorporated into the valence orbitals. Both molecular and dissociative configurations of the adsorbate H_2O are considered at one molecular layer coverage. For molecular water adsorption, LDA calculations indicate binding only at the top site, whereas the GGA indicates no binding for any site. Dissociative adsorption is found to be energetically more favorable than molecular adsorption, in agreement with experimental observations. The effects on the geometric and electronic structures influenced by water adsorption are investigated.

DOI: 10.1103/PhysRevB.65.085403

PACS number(s): 82.65.+r, 71.15.Mb, 71.15.Dx

I. INTRODUCTION

Characteristics of water adsorption on solid surfaces have received widespread attention in many areas of research such as heterogeneous catalysis, environmental protection, and corrosion, to name a few.¹⁻⁴ In particular, the surfaces of plutonium dioxide are chemically active, resulting in strong interactions with adsorbates. The interactions of these surfaces with water are rather important from scientific and technological points of view. The scientific importance partly originates from the complex behavior of the f electrons, while the technological relevance is related to the safe extended storage of the oxide and other environmental issues.⁵⁻⁷ We first comment on the published literature.

Experimental observations of water adsorption on PuO_2 are well documented.^{1,8-15} We specifically comment on three of these publications. Stakebake and Steward¹ measured gravimetrically adsorption isotherms of water vapor on plutonium dioxide at 30, 50, and 85 °C. A three-step model for the total adsorption process was proposed consisting of surface hydroxylation (chemisorption), hydrogen bonding of water molecules to surface hydroxyls (quasichemisorption), and physisorption of water molecules. Combined with mass-time data extracted from literature sources, an extensive investigation of kinetic and equilibrium properties of water adsorption by PuO_2 were carried out by Haschke and Ricketts¹³ from gravimetric measurements in moist air at room temperature. Results suggest that water is accommodated by a sequence of distinct steps involving five types of adsorbate-oxide surface interactions ranging from strong dissociative chemisorption to molecular condensation and accumulating ten molecular layers of water. The humidity-dependent first and second steps involve half molecular layers of water, and are attributed to dissociative chemisorption of water as OH. Haschke *et al.*¹⁵ investigated the chemical and kinetic behavior of the gas-oxide systems over the 25–250 °C range using pressure-volume-temperature and microbalance methods. The results indicated that water adsorbed strongly on the oxide below 120 °C, and desorbed as the temperature was increased to 200 °C. Hydroxide formed by dissociative adsorption of water promoted formation of

the higher oxide of plutonium, PuO_{2+x} and H_2 .

Although there are significant experimental studies of water adsorption on PuO_2 , no theoretical study has been published to the best of our knowledge. In this paper, as an attempt to investigate this highly complex problem, we have applied the techniques of modern density-functional theory (DFT) with relativistic effective core potentials (ECPs) to investigate the geometric and electronic characteristics of water adsorption on a $\text{PuO}_2(110)$ surface at one molecular layer coverage. A periodic model has been used to study the possibilities of different adsorption processes, namely, molecular adsorption and dissociative adsorption.

II. COMPUTATIONAL DETAILS AND RESULTS

As in our previous studies on the electronic properties of both bulk PuO_2 and its (110) surface,⁷ all the computations reported here have been carried out on a 16-processor SGI/CRAY Origin 2000 supercomputer using the DFT package *DMOL*³ (Ref. 16) in the *CERIUS*² program suite.¹⁷ Numerical spin unrestricted density, functional calculations were performed at both local-density-approximation (LDA) (Ref. 18) and generalized-gradient-approximation (GGA) (Ref. 19) levels. Double numerical basis sets with polarization functions (DNP's) are used for both oxygen and plutonium. The sizes of these DNP basis sets are comparable to the 6-31G** basis set of Hehre *et al.*²⁰ However, they are believed to be much more accurate than a Gaussian basis set of the same size.^{16,17} A relativistic ECP with a small [Kr] $4d^{10}4f^{14}$ core is used for plutonium.²¹ The remaining 34 electrons (including and beyond the fifth shell) are treated as valence electrons. The scalar relativistic approach employed here was developed by Wood and Boring.²² Mass-velocity and Darwin terms are added to the nonrelativistic Hartree-Fock operator. However, spin-orbit coupling is not explicitly included in this approach. Although the ECP's are developed from Hartree-Fock calculations, it has been demonstrated that they can be used in DFT-based methods as well.²³ It is expected that the effects of spin-orbit coupling are not very significant. Hay and Martin,²⁴ for example, found that one could adequately describe the electronic and geometric prop-

erties of PuO_2^+ containing actinide species without treating spin-orbit effects explicitly. Similar conclusions have been reached by us in our study of molecular PuO_2 and PuN_2 , and by Ismail *et al.* in their study of uranyl and plutonyl ions.²⁵

Before considering water adsorption, we first studied the clean $\text{PuO}_2(110)$ surface. As is known, fluorite-type bulk PuO_2 has a structure of CaF_2 with a lattice constant of $5.396 \pm 0.002 \text{ \AA}$, where plutonium forms a face-centered-cubic sublattice inside which there is a simple cubic sublattice of oxygen.²⁶ Preferential cleavage of fluorite occurs parallel to the (110) and (111) planes and the surface contains twice as many oxygen atoms compared to plutonium atoms.¹³ As measures of the accuracy of the approximations used in this work, we note that Perdew and Wang's local functional,¹⁸ which gives binding energy of 20.36 eV compared to the experimental value of 19.72 eV,²⁷ results in a shorter lattice constant of 5.30 \AA . The cohesive or binding energy E_c is determined experimentally by measuring the heat of formation H of PuO_2 (starting with Pu metal and O_2 molecules), the sublimation energy S of Pu metal, and the dissociation energy D of O_2 . Thus $E_c = S + D - H$. The non-local functional,¹⁹ on the other hand, underestimates the binding energy as 17.28 eV and gives a lattice constant of 5.34 \AA .⁷ The $\text{PuO}_2(110)$ surface here is modeled by a five-layer slab unit cell cleaved from the bulk structure (Fig. 1), which contains five nonequivalent Pu atoms and ten oxygen atoms. The thickness of the vacuum layers has been chosen to be 15 \AA , and, as mentioned above periodic boundary conditions have been applied in the calculations. The sampling of the Brillouin zone is restricted to the Γ point, and both the interlayer separations between the Pu atoms as also the positions of the O atoms are optimized at the LDA and GGA levels. The maximum number of numerical integration mesh points available in *DMOL*³ has been chosen for the computations, and the threshold of the density-matrix convergence is set to 10^{-5} . The optimization gradient convergence is set to 10^{-3} Hartree/Bohr. In general, the optimization procedure yielded rather small changes relative to the ideally terminated bulk geometry, with both LDA and GGA results showing an inward relaxation. With respect to the ideal positions of plutonium atoms, the surface layers (the first and fifth layers) are contracted by 6.3% and 9.1% for the GGA and LDA, respectively, leaving the two oxygen atoms out of the surface by 0.13 \AA (7.3% of the new interlayer distance) and 0.11 \AA (i.e., 6.9% of the interlayer distance), respectively.

The other interlayer distances remain the same as the ideal surface terminated from the bulk. The distance between the two oxygen atoms on the top layers are found to increase by 5.2% and 6.4%, for the GGA and LDA, respectively. This indicates the possibility of dimer formation between the oxygen atom and its nearest-neighbor oxygen in the next cell. The surface relaxation energy, defined by the difference between the total energy of the unrelaxed and relaxed surfaces, is found to be 0.53 and 1.15 eV per unit cell for the GGA and LDA, respectively. The results are summarized in Table I, and are consistent with our previous results,⁷ where only first-layer relaxation and reconstruction using the GGA were considered. However, the magnitude of the surface relaxation energy is doubled compared to our previous results.⁷ We be-

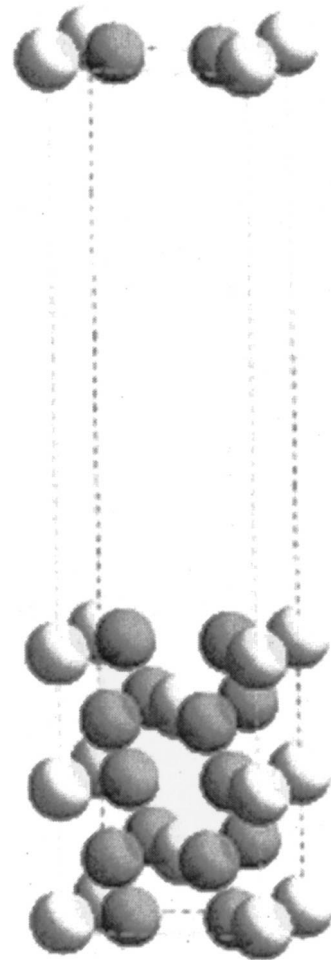


FIG. 1. Unit cell of the $\text{PuO}_2(110)$ surface, where the dark gray balls are oxygen atoms and the light gray balls are plutonium atoms.

lieve that this is due to full optimization and relaxation of both surface layers.

In the next stage of the calculations, we studied molecular water adsorption on the $\text{PuO}_2(110)$ surface at monolayer coverage, i.e., one water molecule per unit cell, containing one nonequivalent plutonium and two oxygen atoms on the top layer. The four possible adsorption sites considered here are illustrated in Fig. 2, where *A* is the top site on Pu, *B* is the long bridge site between two oxygen atoms in the same cell, *C* is the cave site, and *D* is the short bridge site between two oxygen atoms from neighboring cells. Again, geometry optimizations have been performed for water adsorption on each site in the molecular configuration. Experimental observation shows that hydrogen is the only gaseous product formed during exposure of plutonium dioxide to water,⁹ indicating a relatively strong interaction between O and the surface; therefore, we only considered the configuration of water adsorption with its oxygen atom heading to the surface. The significantly stronger Pu-O interactions over Pu-H and O-H interactions were also confirmed by an approach using thermodynamic data for water,²⁸ and for compounds of plutonium with oxygen²⁹ and hydrogen.³⁰

The adsorption energy and the optimized geometry parameters are listed in Table 1 and are compared to the corre-

TABLE I. Adsorption energy (eV) and geometry parameters (distance in Å and angle \angle HOH in degrees) for water adsorbed on a $\text{PuO}_2(110)$ surface and geometry parameters for the relaxed and ideal surfaces. Here h_{ij} is the interlayer distance between the i th layer and the j th layer; $h_{\text{Pu-Os}}$ is the vertical distance between Pu and O in the top layer; d_{OO} is the distance between the two oxygen atoms in the top layer. $h_{\text{Ow-Pu}}$ is the vertical distance between the O in water and the top layer; d_{OH} is the bond length of O and H in the water molecule.

Site	E_{bind}	h_{12}	h_{23}	h_{34}	h_{45}	$h_{\text{Pu-Os}}$	d_{OO}	$h_{\text{Ow-Pu}}$	\angle HOH	d_{OH}
GGA										
A (top)	-0.096	1.70	1.95	1.97	1.67	0.10	2.82	2.55	107.7	0.98
B (bridge l)	-0.452	1.68	1.96	1.97	1.68	0.11	2.82	4.85	104.9	0.97
C (cave)	-0.455	1.69	1.96	1.97	1.68	0.11	2.82	3.68	104.3	0.97
D (bridge s)	-0.341	1.69	1.95	1.97	1.67	0.09	2.81	3.56	103.7	0.96
Dissociative configuration						0.25				0.97
Relaxed surface	0.013	1.84	1.88	2.00	1.66	0.06	2.80	2.10	126.0	2.38
Ideal surface	—	1.77	1.89	1.89	1.77	0.13	2.81	—	—	—
Free H_2O	—	—	—	—	—	—	—	—	104.2	0.97
LDA										
A (top)	0.172	1.62	1.85	1.88	1.60	0.08	2.82	2.42	108.9	0.98
B (bridge l)	-0.499	1.59	1.88	1.87	1.60	0.09	2.84	2.51	105.4	0.97
C (cave)	-0.373	1.60	1.88	1.87	1.60	0.11	2.85	1.82	104.5	0.98
D (bridge s)	-0.296	1.63	1.86	1.88	1.60	0.05	2.81	2.82	104.3	0.97
Dissociative configuration						0.18				0.97
Relaxed surface	0.494	1.73	1.81	1.90	1.58	0.02	2.81	2.00	120.8	2.25
Ideal surface	—	1.60	1.87	1.87	1.60	0.11	2.82	—	—	—
Free H_2O	—	—	—	—	—	—	—	—	104.9	0.97

sponding data of the relaxed and ideal surfaces. Compared to the geometry data of the free water molecule, neither the bond angle nor the O-H bond length of the adsorbate H_2O has a significant change for most of the sites considered here. However, noticeable change of the bond angle can be seen for adsorption on the top site. The adsorption energy is calculated with respect to the clean slab and the water molecule in vacuum, with positive values indicating binding. As can

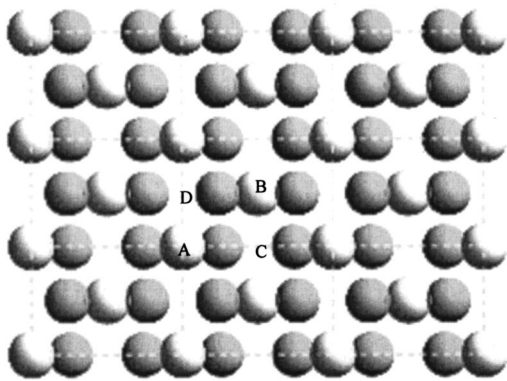


FIG. 2. Top view of the $\text{PuO}_2(110)$ surface. A–D denote adsorption sites of water molecules. The dark gray balls are oxygen atoms and the light gray balls are plutonium atoms.

be seen from the table, only at the LDA level of theory, we have a positive adsorption energy of 0.172 eV, and this occurs for the top site [Fig. 3(a)]. On a relative scale, top site is the energetically favorable site for water adsorption followed by the short bridge site for both levels of theory. This can be understood by the fact that, in the bulk geometry, each plutonium atom sits in a fragment of the eightfold cubic coordination geometry of oxygen atoms. When the surface is

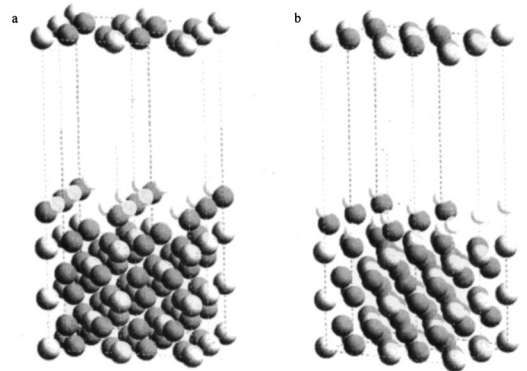


FIG. 3. Water adsorption on the $\text{PuO}_2(110)$ surface. (a) Molecular configuration; (b) Dissociative configuration; the dark gray balls are oxygen atoms, the light gray balls are plutonium atoms, and the small white balls are hydrogen atoms.

cleaved from the bulk, the dangling bond of the plutonium atom on the top layer will attract the foreign oxygen. The discrepancy of the LDA and GGA results regarding to the sign of the adsorption energy can be understood by the fact that usually the LDA tends to give overbinding, while the GGA underestimates binding. For weakly bound systems dispersion, the major mechanism for physical interactions, is not fully covered by the current correlation functionals.³¹ The overbinding nature inherent in the LDA, however, somewhat compensates for the lack of dispersion. Therefore, at this point, we can only conclude that, at this low coverage, the physisorption of water molecules on the $\text{PuO}_2(110)$ surface is not favored. This is consistent with experimental observations.¹³

In the next step, we studied water adsorption in a dissociative configuration. Guided by previous results, we considered adsorption only for the top site in a bond-broken configuration. The adsorption energies are found to be 0.494 and 0.013 eV at LDA and GGA levels, respectively. Compared to the adsorption energies in the molecular configuration, both LDA and GGA results show that dissociative adsorption is more favorable than molecular adsorption. Full geometry optimization indicates that in this bond-broken configuration, OH is adsorbed on Pu, while the other hydrogen is bonded to a surface oxygen [Fig. 3(b)]. This is consistent with experimental observations that water adsorption on PuO_2 at low coverage (0.5–1 ML) is dissociative.^{1,8–15} We note that the GGA gives a rather weak binding of only 0.013 eV, compared to the LDA value of 0.494 eV. The weak binding energy could again be attributed to the fact that the long range correlations (i.e., dispersion) are not fully accounted for in the present correlation functionals.³¹ However, we note good qualitative agreements with experimental results.

We also studied the influences of the adsorbate H_2O on the geometry of the plutonium dioxide surface. The results are summarized in Table I. For the configuration of molecular adsorption, LDA results show no noticeable change on the surface geometry by adding water molecules on any of the sites. Conversely, GGA results show that adding water molecules on each site makes the surface layers (the first and fifth layers) contract further while the inner layers expand. Comparing to the relaxed free surface slab, both the contraction and expansion are about 4%. For the configuration of dissociative adsorption, on the other hand, the GGA and LDA give very similar results. The bond lengths of O and H in the water molecule are found to be 0.97 and 2.38 Å with a bond angle of 126.0° for the GGA. For the LDA, the bond lengths are 0.97 and 2.25 Å, with a bond angle of 120.8°. Compared to the relaxed clean surface slab, both GGA and LDA results show that the top layer expands while the fifth layer contracts (here water is only adsorbed on the top layer). We also find that the distance h_{34} between the third and fourth layers increases by 6% for the GGA, while the distance h_{23} between the second and third layers remains almost unchanged. However, LDA results show that the distance h_{12} decreases by 3%, while h_{34} increases by 2%. It is interesting to note that the surface oxygen atom, which is bonded to the hydrogen atom from a broken water molecule, is dragged out

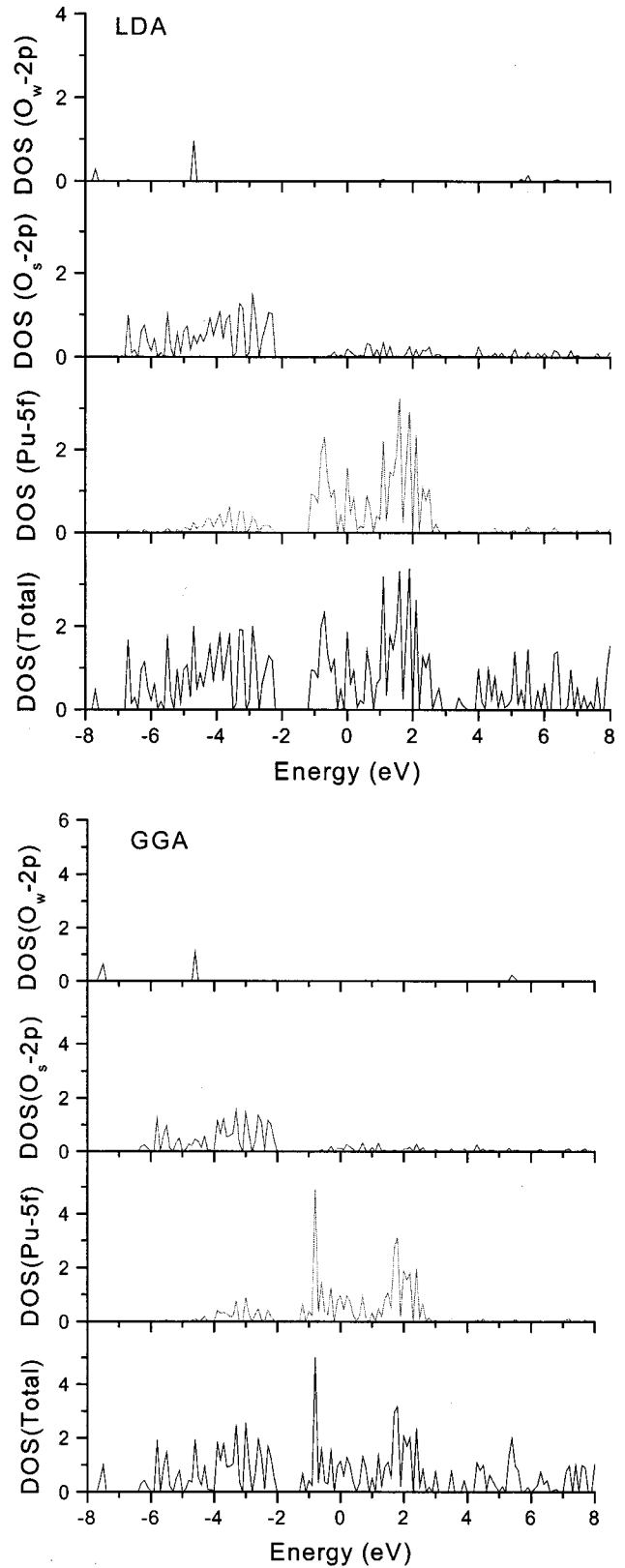
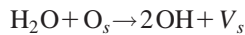


FIG. 4. Density of states, with corresponding O 2p and Pu 5f components, of a $\text{PuO}_2(110)$ surface as well as the components from the O 2p in the adsorbate H_2O for water molecule adsorbed on the top site. The energy of the HOMO is set to zero.

TABLE II. Mulliken analysis for the spin densities and effective charges carried by Pu and O atoms on different layers for both free and water-adsorbed PuO₂ (110) surfaces for the top site in both molecular and dissociative configurations, as well as spin and charges carried by H and O atoms in both free and adsorbate water molecules.

GGA		Free surface or H ₂ O		H ₂ O adsorbed on the top site in molecular configuration		H ₂ O adsorbed on the top site in dissociative configuration	
Layer	Element	charge	spin	charge	spin	charge	spin
1	Pu	0.80	4.48	0.88	4.39	0.88	4.31
	O	-0.57	-0.23	-0.57	-0.22	-0.58	-0.09
2	Pu	1.43	4.29	1.43	4.26	1.42	4.29
	O	-0.61	-0.14	-0.61	-0.14	-0.60	-0.15
3	Pu	1.46	4.27	1.47	4.25	1.46	4.28
	O	-0.60	-0.18	-0.60	-0.18	-0.61	0.17
4	Pu	1.43	4.29	1.42	4.29	1.41	4.29
	O	-0.61	-0.14	-0.61	-0.14	-0.61	-0.14
5	Pu	0.80	4.48	0.77	4.49	0.79	4.49
	O	-0.57	-0.23	-0.58	-0.22	-0.58	-0.22
LDA							
H ₂ O	O	-0.52	0.00	-0.42	-0.02	-0.58	-0.07
	H	0.26	0.00	0.19	0.07	0.23	0.00
	H	0.26	0.00	0.19	0.07	0.34	0.01
1	Pu	0.72	4.44	0.83	4.32	0.82	4.22
	O	-0.57	-0.17	-0.56	-0.17	-0.58	-0.06
2	Pu	1.44	4.15	1.43	4.10	1.43	4.18
	O	-0.61	-0.10	-0.61	-0.10	-0.61	-0.11
3	Pu	1.56	4.16	1.55	4.14	1.53	4.18
	O	-0.59	-0.13	-0.59	-0.13	-0.60	-0.12
4	Pu	1.44	4.14	1.43	4.15	1.42	4.15
	O	-0.61	-0.10	-0.61	-0.10	-0.62	-0.10
5	Pu	0.72	4.44	0.70	4.45	0.72	4.45
	O	-0.57	-0.17	-0.58	-0.17	-0.58	-0.17
H ₂ O	O	-0.56	0	-0.43	-0.04	-0.58	-0.04
	H	0.28	0	0.19	0.11	0.26	0.00
	H	0.28	0	0.19	0.11	0.36	0.01

of the surface by 0.25 Å for the GGA and 0.18 Å for the LDA (i.e., 13.6% and 10.4% of the corresponding interlayer distance for the GGA and LDA, respectively), while the other surface oxygen atom is pushed below the surface by 0.06 and 0.02 Å, for the GGA and LDA, respectively. This supports the idea¹³ that the dissociative adsorption of water involves reaction of water with surface oxygen O_s as described by



where V_s is a vacancy formed by removing oxygen from a tetrahedral-fragment site at the oxide surface.

To understand the reasons for the geometry changes induced by water adsorption, we also performed a Mulliken population analysis³² to compute the effective charges and spin densities carried by Pu and O atoms, as well as those carried by O and H atoms in a water molecule for both the free surface or H₂O and the water-adsorbed surface in both configurations. The results are summarized in Table II. We

first note that from the charges carried by Pu and O for both surface slabs, the chemical bonding between O and Pu is not ideally ionic. Each layer is charged, though the whole unit cell remains neutral. The two surface layers are negatively charged, while the three inner layers are positively charged. Both LDA and GGA results show that with water adsorbed on the surface in both configurations, only Pu on the first layer becomes even more positively charged, while charges on other atoms in the slab are not noticeably changed. This indicates that the interactions between the adsorbate H₂O and the surface are fairly weak, and only occur through interactions with the Pu on the top layer. However, for molecular adsorption, the adsorbate H₂O now carries negative charges, which is partially responsible for the expansion of the positively charged inner layers. We also note that the fifth layer gains $-0.04e$ that makes itself relaxed more inward. If one considers dissociative adsorption, major differences can be noted for the effective charges carried by the O and H atoms in the adsorbate. The hydrogen atom which is bonded

to the surface oxygen O_s , carries more positive charges, i.e., $0.34e$ for the GGA and $0.36e$ for the LDA, respectively, which indicates the fairly strong interaction with the surface oxygen. Due to the bond breaking of the water molecule, the adsorbate oxygen atom gained more charges from the surface, which explains the stronger binding in this configuration. The high-spin densities possessed by Pu atoms show the magnetic characteristics for this system. However, water adsorption does not have much influence on the spin densities.

Finally, in Fig. 4 we plot the density of states (DOS) for the $PuO_2(110)$ surface with water adsorbed on the top site in the dissociative configuration. A gaussian broadening procedure has been employed here to compute the DOS. As done in our previous studies,⁷ a Gaussian $\exp(-\alpha x^2)$ is assigned to each molecular-orbital eigenvalue with $\alpha=1000$, such that the width at the half height is 0.05 eV. The DOS at each energy point comes from the contributions of all the molecular orbitals. The DOS's from both LDA and GGA calculations show metallic features of the water-adsorbed surface. The conduction bands around the Fermi level are dominated by the Pu $5f$ states. On the other hand, the valence bands are mostly from the surface O $2p$ states, with small contributions from both Pu $5f$ states and O $2p$ states of the adsorbate water.

In summary, we have performed both LDA and GGA computations for the geometric and electronic structures off $PuO_2(110)$ surface, with water adsorbed on four different sites in a molecular configuration and at one molecular coverage. LDA data indicates that the Pu top site is the energetically favorable site for water adsorption. On the other hand, at the GGA level, all the binding energies are negative, implying that molecular water adsorption does not occur. We further studied the possibility of dissociative adsorption on the Pu top site. Both GGA and LDA results here show that dissociative adsorption is energetically more favorable than molecular adsorption. This is in agreement with experimental observations that water adsorption on PuO_2 at low coverage is dissociative.

ACKNOWLEDGMENTS

This work was partially supported by the Welch Foundation, Houston, Texas (Grant No. Y-1525) and by the Amarillo National Research Center, Amarillo, Texas through a Cooperative Agreement (No. DE-FC04-95AL85832) with the U.S. Department of Energy.

*Email address: akr@exchange.uta.edu

- ¹J. L. Stakebake and L. M. Steward, *J. Colloid Interface Sci.* **42**, 328 (1973).
- ²M. Odelius, M. Bernasconi, and M. Parrinello, *Phys. Rev. Lett.* **78**, 2855 (1997).
- ³E. V. Stefanovich and T. N. Truong, *Chem. Phys. Lett.* **299**, 623 (1999).
- ⁴M. Odelius, *Phys. Rev. Lett.* **82**, 3919 (1999).
- ⁵S. S. Hecker, in *Plutonium Futures-The Science*, edited by K. S. Pillay and K. C. Kim, AIP Conf. Proc. No. 532 (AIP, New York, 2000), p. 6.
- ⁶*Challenges in Plutonium Science*, Vols. I and II, Los Alamos Science, Number 26, 2000.
- ⁷X. Wu, Ph.D. thesis, The University of Texas at Arlington, 2001; X. Wu and A. K. Ray, *Physica B* **293**, 362 (2001); **301**, 359 (2001); *Eur. Phys. J. B* **19**, 345 (2001).
- ⁸L. A. Morales, J. M. Haschke, and T. H. Allen, U.S. DOE Report No. LA-13597-MS, Los Alamos National Laboratory, Los Alamos, NM, May 1999.
- ⁹J. M. Haschke and T. H. Allen, U.S. DOE Report No. LA-13537-MS, Los Alamos National Laboratory, Los Alamos, NM, January 1999.
- ¹⁰J. M. Haschke and T. E. Ricketts, U.S. DOE Report No. LA-12999-MS, Los Alamos National Laboratory, Los Alamos, NM, August 1995.
- ¹¹J. L. Stakebake, D. T. Larson, and J. M. Haschke, *J. Alloys Compd.* **202**, 251 (1993).
- ¹²J. M. Haschke, T. H. Allen, and L. A. Morales, *J. Alloys Compd.* **243**, 23 (1996).
- ¹³J. M. Haschke and T. E. Ricketts, *J. Alloys Compd.* **252**, 148 (1997).
- ¹⁴L. Morales, T. Allen, and J. Haschke, in *Plutonium Factors—The Science* (Ref. 5), p. 114.

- ¹⁵J. M. Haschke, T. H. Allen, and L. A. Morales, *J. Alloys Compd.* **314**, 78 (2001).
- ¹⁶B. Delley, *J. Chem. Phys.* **92**, 508 (1990); A. Kessi and B. Delley, *Int. J. Quantum Chem.* **68**, 135 (1998); B. Delley, *ibid.* **69**, 423 (1998); *J. Chem. Phys.* **113**, 7756 (2000).
- ¹⁷*DMol³-Cerius²/Quantum Chemistry*, Release 3.8, MSI, San Diego, 1998.
- ¹⁸J. P. Perdew and Y. Wang, *Phys. Rev. B* **45**, 13 244 (1992).
- ¹⁹J. P. Perdew and Y. Wang, *Phys. Rev. B* **46**, 12 947 (1992); **46**, 6671 (1992).
- ²⁰W. J. Hehre, L. Radom, P. v. R. Schleyer, and J. A. Pople, *Ab Initio Molecular Orbital Theory* (Wiley, New York, 1986).
- ²¹W. Kuchle, M. Dolg, H. Stoll, and H. Preuss, *J. Chem. Phys.* **100**, 7535 (1994).
- ²²J. H. Wood and A. M. Boring, *Phys. Rev. B* **18**, 2701 (1978).
- ²³T. V. Russo, R. L. Martin, and P. J. Hay, *J. Phys. Chem.* **99**, 17085 (1995).
- ²⁴P. J. Hay and R. L. Martin, *J. Chem. Phys.* **109**, 3875 (1998).
- ²⁵E. F. Archibong and A. K. Ray, *J. Mol. Struct.: THEOCHEM* **530**, 165 (2000); N. Ismail, J.-L. Heully, T. Saue, J.-P. Daudey, and C. J. Marsden, *Chem. Phys. Lett.* **300**, 296 (1999).
- ²⁶I. Narai-Szabo, *Inorganic Crystal Chemistry* (Academia Kiado, Budapest, 1969); U. Benedict, G. D. Andreotti, J. M. Fournier, and A. Waintal, *J. Phys. (France) Lett.* **43**, L171 (1982); U. Benedict and W. B. Holzapfel, *Handbook on the Physics and Chemistry of Rare Earths*, Vol 17, p. 245 (1993); N. V. Dedov and V. F. Bagryantsev, *Radiochemistry* **38**, 24 (1996).
- ²⁷K. P. Huber, in *American Institute of Physics Handbook* (McGraw-Hill, New York, 1972), Sec. 7(g); L. R. Morss, J. Less-Common Met. **93**, 301 (1983); P. J. Kelly and M. S. S. Brooks, *J. Chem. Soc., Faraday Trans. 2* **83**, 1189 (1987).
- ²⁸*JANAF Thermochemical Tables*, NSRDS-NBS 37, U.S. Depart-

- ment of Commerce, National Bureau of Standards, Washington, D.C., 2nd ed., 1971.
- ²⁹*The Chemistry of the Actinide Elements*, edited by L. R. Morss, in J. J. Katz, G. T. Seaborg, and L. R. Morse (Chapman and Hall, New York, 1986), Chap. 17.
- ³⁰*The Chemical Thermodynamics of Actinide Elements and Compounds*, edited by H. E. Flotow, J. M. Haschke, S. Yamauchi, and F. L. Oetting (International Atomic Energy Agency, Vienna, Austria, 1984), pt. 9.
- ³¹X. Wu, M. C. Vargas, S. Nayak, V. F. Lotrich, and G. Scoles, *J. Chem. Phys.* **115**, 8748 (2001).
- ³²R. S. Mulliken, *J. Chem. Phys.* **23**, 1833 (1955); **23**, 1841 (1955); **23**, 2338 (1955); **23**, 2343 (1955).